Liu et al., J Proteomics Bioinform 2019, 12:1
DOI: 10.4172/0974-276X.1000490

Journal of
Proteomics & Bioinformatics

Research Article Open Access

Redox Proteome Perturbation in Arabidopsis upon *Pseudomonas syringae* Infection

Pei Liu[1], Huoming Zhang[2]*, Liming Xiong[3] and Yiji Xia[4]*

[1]*Proteomics Center, University of Missouri, Columbia, MO 65212, USA*
[2]*Core Labs, King Abdullah University of Science and Technology, Thuwal, 23955-6900 Saudi Arabia*
[3]*Department of Horticultural Sciences, Texas A&M University, College Station, TX 77843, USA*
[4]*Department of Biology, Hong Kong Baptist University, Hong Kong SAR, China*

Abstract

Oxidative burst is one of the earliest plant cellular responses triggered by pathogen infection. Reactive oxygen species can cause oxidative modifications of redox-sensitive proteins to mediate the defense responses. Identification and characterization of proteins that undergo oxidative modifications in these processes is an important step toward understanding molecular mechanisms of plant defense responses. In this study, an *in vivo* 15N metabolic labeling method combined with a cysteine-containing peptide enrichment technique was applied to identify and quantify proteins and their redox states in Arabidopsis in response to infection by *Pseudomonas syringae* pv *tomato* DC3000 (*Pst*). Changes of peptide redox states were compared and corrected with the changes of protein levels. A total of forty peptides representing thirty-six non-redundant proteins showed significantly redox state changes in response to the infection by the virulent *Pst* strain and the avirulent *Pst* strain (*Pst avrRpm1*), of which 23 had previously not been recognized to undergo oxidative PTMs. The differentially expressed redox-sensitive proteins are involved in cell wall organization, primary metabolism, photosynthesis and stress responses. Interestingly, proteins located at extracellular were more susceptible to be regulated on the redox PTMs level. These findings provide a foundation for further investigation into the redox signaling during plant defense responses.

Keywords: 15N metabolic labeling; Redox-sensitive proteins; Arabidopsis; Pathogen

Abbreviations: ROS: Reactive Oxygen Species; PAMPs: Pathogen Associated Molecular Patterns; PTI: PAMP-Trigged Immunity; ETI: Effector-Triggered Immunity; *Pst*: *Pseudomonas syringae* pv *tomato* DC3000; NEM: N-Ethylmaleimide; biotin-HPDP: N-[6-(Biotinamido) hexyl]-3'-(2'-pyridyldithio) propionamide; ACN: Acetonitrile; CID: Collision Induced Dissociation; MGF: Mascot Generic Format; TPP: Trans-Proteomic Pipeline; DAB: Diaminobenzidine; BGALs: Beta Galactosidases; AtLDA: Limit Dextrinase; HCF101: High Chlorophyll Fluorescence 101; UVR8: UV Resistance Locus 8; PTMs: Post-Translational Modifications

Introduction

Plants frequently encounter a wide range of pathogenic microbes such as bacteria, fungi, oomycetes, and viruses. The rapid activation of plant's innate immune system is necessary for successful pathogen resistance [1]. The outcome of the plant-pathogen interaction is dependent on different types of pathogens and the genetic constitution of the hosts [2]. The initial host response is activated when host cells recognize pathogen-associated molecular patterns (PAMPs), which is termed PAMP-trigged immunity (PTI). Pathogens use various effector proteins encoded by avirulent genes to suppress PTI to facilitate their infection. In turn, plants have evolved many RESISTANCE (R) proteins, each of which can recognize one or more specific effectors to induce effector-triggered immunity (ETI) which is a strong response often leading to programmed cell death in the infected sites [3]. Pathogen strains that can avoid ETI and successfully colonize hosts are often called virulent strains, whereas those stains whose effector protein triggers ETI and fail to establish successful infection are termed avirulent strains [4]. The bacterial pathogen *Pseudomonas syringae* is a widely used pathogen in laboratory experiments to study Arabidopsis's defense responses.

The production of reactive oxygen species (ROS) in a so-called oxidative burst is one of the plant' early defense reactions to pathogen attack [5]. An initial weak oxidative burst can be detected following infection by either a virulent or avirulent strain. During the incompatible plant-pathogen interaction following attack by an avirulent strain, ROS production occurs in a biphasic manner with a weak oxidative burst followed by a second and massive oxidative burst [6]. The initial oxidative burst is believed to be triggered by PTI. Indeed, an oxidative burst was recorded in Arabidopsis within a few minutes of perception of flg22, a 22 amino acid peptide from bacterial pathogens flagellin that acts as a PAMP [7]. The second strong burst is induced during ETI. Furthermore, H_2O_2 generation occurs both locally and systemically in response to pathogen infection [8]. H_2O_2 and other ROS are well recognized as a second messenger for the activation of local and systemic expression of defense genes and other defense mechanisms in plants [9].

The signaling role of ROS is largely achieved through chemoselective oxidative modifications of cellular molecules, thereby altering protein activities and functions [10]. Proteins containing cysteines are particularly susceptible to oxidation in different forms due to a low pKa sulhydryl group of cysteine [11]. Many redox-sensitive proteins have been identified in plants that might play important roles in sensing cellular redox status and transducing redox signals into physiological responses [12-16]. A limited number of defense-related proteins have been shown to be redox-regulated in plants, such as non-expressor of PR-1 (NPR1) [17], TGACG sequence-specific binding protein 1 (TGA1) [18], NADPH oxidase [19], salicylic acid-binding protein 3

***Corresponding author:** Huoming Zhang, Core Labs, King Abdullah University of Science and Technology, Thuwal, 23955-6900 Saudi Arabia, Tel: +966128082518; E-mail: huoming.zhang@kaust.edu.sa

Yiji Xia, Department of Biology, Hong Kong Baptist University, Hong Kong SAR, China, Tel: +85234117052; E-mail: yxia@hkbu.edu.hk

Received December 14, 2018; **Accepted** January 05, 2018; **Published** January 14, 2019

Citation: Liu P, Zhang H, Xiong L, Xia Y (2019) Redox Proteome Perturbation in Arabidopsis upon *Pseudomonas syringae* Infection. J Proteomics Bioinform 12: 001-009. doi: 10.4172/0974-276X.1000490

(AtSABP3) [20], serine–threonine receptor kinase and 3-ketoacyl-CoA thilase (KAT2) [21]. In recent years, redox proteomics techniques have been used to identify redox-sensitive proteins that undergo oxidative modifications in response to various stimuli [22,23]. However, such an approach has not been reported in identifying proteins that alter redox states upon virulent and avirulent pathogen infection in Arabidopsis plants.

In this study, we applied a biotin-switch method and stable isotope nitrogen (^{15}N) metabolic labeling to identify redox-sensitive proteins during plant-pathogen interaction, in which the cysteine-containing peptides were enriched followed by identification and quantification using mass spectrometric analysis. In total, 387 cysteine-containing peptides were identified upon the infection by the virulent strain *Pseudomonas syringae* pv *tomato* DC3000 (*Pst*) and the isogenic avirulent strain *Pst avrRpm1*. After being normalized to the total protein expression level, thirty-six proteins were found to have significant change in their redox states upon the pathogen infection.

Materials and Methods

Plant material and growth condition

Wild-type *Arabidopsis thaliana* Col-0 seeds were grown in the solid medium containing 1/2 Murashige and Skoog basal salt micronutrient solution (sigma), 1.5 mM $CaCl_2$, 0.75 mM $MgSO_4$, 0.625 mM KH_2PO_4, 9.4 mM KNO_3, 10.3 mM NH_4NO_3, 0.5 g/L MES, 1% sucrose, pH 5.7 with 0.6% (w/v) Agar. The 15N-labeled media was prepared using 98% ammonium nitrate-$^{15}N_2$ and potassium nitrate-^{15}N (sigma) in place of natural abundance of nitrogen salts (^{14}N) as the only nitrogen source. Plants were grown in a growth chamber under a 16-hour light/8-hour dark cycle at 23 °C for 3 weeks.

Pathogen infection

The virulent strain *Pseudomonas syringae* pv *tomato* DC3000 (*Pst*) and the isogenic strain carrying the avirulence gene *avrRpm1* (*Pst avrRpm1*) [24] were grown on the King's B medium plates containing kanamycin and rifamycin antibiotics at 30°C for 48 hours. Bacteria were then restreaked onto new plates and grown for another 24 hrs. The new freshly streaked bacteria was scraped off, resuspended, and diluted to OD600=0.2 (1×10^8 colony-forming units/mL) in sterile 10 mM $MgCl_2$ solution with 0.02% Silwet L-77. More than twenty three-week old plants were sprayed with the prepared bacterial suspension. For the mock treatment, only 10 mM $MgCl_2$ solution with 0.02% Silwet L-77 was used. The bacterial suspension was sprayed onto leaves until there was imminent runoff. For the first biological replicate, ^{15}N-labeled plants were treated with pathogen while ^{14}N plants were treated with the mock. In a reciprocal replicate, ^{15}N-labeled plants were treated with mock while ^{14}N plants were treated with pathogen. After 1 hr and 3 hrs treatment, leaves were harvested, immediately frozen in liquid nitrogen, and ground into a fine powder in prechilled mortar and pestle.

Detection of reactive oxygen species

In situ detection of hydrogen peroxide was performed by staining with DAB (Sigma-Aldrich) as described previously [25]. Briefly, plants were sprayed with *Pst avrRpm1* or *Pst* at OD_{600} = 0.2. After 30 min, 1 hr, 2 hrs, 3 hrs, and 4 hrs, the leaves were collected and infiltrated under gentle vacuum for 5 min with 1 mg/mL DAB containing 0.05% v/v Tween 20 and 10 mM sodium phosphate buffer (pH 7.0). Three leaves per plant from 6 independent plants were used for biological replicates. The experiment was repeated twice. After staining for 5 hrs, the leaves were fixed in ethanol:glycerol:acetic acid 3:1:1 (bleaching solution) in a boiling water bath for 15 min. New bleaching solution was added and leaves were incubated until the chlorophyll was completely bleached. Pictures were taken and the DAB staining intensity was measured using ImageJ. The staining intensity indicates the amount of H_2O_2.

Protein extraction

Natural-abundance (^{14}N) and ^{15}N-labeled plants were combined at a ratio of 1:1 by weight (powder), and suspended in protein extraction buffer [8 M urea, 20 mM Tris-HCl (pH 7.0), 1 mM EDTA, 1% protease inhibitor cocktail (Sigma-Aldrich, St Louis, MO, USA)] supplemented with 100 mM N-ethylmaleimide (NEM), and incubated at room temperature for 30 min. The homogenate was centrifuged for 15 min at 5,000 × g and 4 °C to remove debris. The proteins from the supernatant were purified using methanol / chloroform precipitation. Precipitated protein pellet was suspended in protein extraction buffer and quantified using 2-D Quant kit (GE Healthcare Life Sciences).

Trypsin digestion and Cysteine-containing peptides purification

Approximately 1 mg protein was reduced by 10 mM DTT at 37 °C for 30 min. The excess DTT was removed by passing though Zeba Spin desalting columns (Thermo Scientific, Rockford, IL, USA) pre-equilibrated with 20 mM Tris-HCl (pH 8.0) and 1 mM EDTA. The protein was then incubated with N-[6-(Biotinamido) hexyl]-3'-(2'-pyridyldithio) propionamide (biotin-HPDP) at a final concentration of 0.4 mM at room temperature for 1 hr. It was diluted to less than 1 M urea using 50 mM ammonium bicarbonate prior to trypsin digestion with 1:40 ratio of trypsin to protein in 37 °C for overnight. TFA was added to a final concentration of 1% (v/v) to stop the digestion. Purification of the biotin-tagged peptides was performed as previously described [15]. For total protein abundance determination, 200 µg protein was reduced by 10 mM DTT at 37 °C for 30 min and alkylated by 55 mM iodoacetamide at RT in the dark for 30 min. The samples were diluted to less than 1 M urea using 50 mM ammonium bicarbonate, followed by digestion with trypsin at a 1:40 trypsin-to-protein mass-ratio at 37 °C for overnight. After digestion was stopped by 1% TFA, peptides were desalted by Sep-Pak C18 cartridges, and dried in a Speed Vac.

Mass spectrometry analysis

The samples were analyzed twice with an LTQ-Orbitrap Velos (Thermo *Scientific*) coupled with a UPLC (Dionex ultimate 3000, Thermo Scientific). The samples were injected and concentrated in a preconditioned Acclaim PepMap100 C18 column (100 µm i.d. fused silica, packed with 5 µm particle size and 300 Å pore size). The peptide separation was performed in a preconditioned Acclaim PepMap100 C18 column (75 um i.d. x 15 cm, 3 µm particle sizes, 100 Å pore sizes). Mobile phase A (0.1% formic acid in H_2O) and mobile phase B (0.1% formic acid in 80% acetonitrile (ACN)) were used to establish a 75-min LC gradient comprised of 55 min of 5-45% B, 5 min of 45-98% B, and 5 min of 98% B. The total flow rate of the gradient was set at 300 nL/min constantly. The samples were introduced into LTQ-Orbitrap through a Nanospray Flex (Thermo Scientific, Germany) with an electrospray potential of 1.5 kV. The ion transfer tube temperature was set at 160 °C. The LTQ-Orbitrap was set to perform data acquisition in the positive ion mode. A full MS scan (350-1600 m/z range) was acquired in the Orbitrap at a resolution of 60,000 (at 400 m/z) in a profile mode, a maximum ion accumulation time of 1 sec and a target value of $1 \times e^6$. Charge state screening for precursor ion was activated. The ten most intense ions above a 1000-count threshold and carrying

multiple charges were selected for fragmentation (MS/MS) in the collision-induced dissociation (CID) in the linear ion trap. Dynamic exclusion for MS/MS fragmentation was activated with a repeat count of 2, repeat duration of 30 sec, exclusion duration of 45 sec, and ±5 ppm mass tolerance. Other settings for CID included a maximum ion accumulation time of 200 ms for MS/MS spectrum collection, a target value of $1 \times e^4$, normalized collision energy at 35%, an activation Q at 0.25, isolation width of 3.0 and activation time of 10 ms.

Database search and data analysis

The raw LC-MS/MS data (*.raw) was converted to mzXML format which was then converted to Mascot Generic Format (MGF,*.mgf) file by Trans-Proteomic Pipeline (TPP, v4.7.1). The MGF file was searched twice with Mascot search engine (v 2.3, Matrix Science) against a concatenated target-decoy Arabidopsis protein database TAIR10 [26], one search with the normal ^{14}N masses and another with ^{15}N masses, respectively. The parameters were set as follows: 10 ppm mass tolerance for peptide masses and 0.5 Da for fragmented ions, a maximum of one missed cleavage for trypsin digestion, fixed modification of carbamidomethylation (57.02) at cysteine, and variable modifications including N-ethylmaleimide (125.05) at cysteine and oxidation (15.99) at methionine. The search result (*.dat) was converted in TPP to pepXML (*.pep.xml) file format. The peptide identification was validated using PeptideProphet and $^{14}N/^{15}N$ peptide ratios were calculated with XPRESS using metabolic labeling 14/15 N approach based on the ^{14}N-^{15}N extracted ion chromatograms area. Peptide and protein probability higher than 0.99 and peptides with an Ion score higher than the Identity score were used for further analysis. Therefore, there was a more than 95% chance that a spectrum peptide sequence match (PSM) was not random [27]. The XPRESS quantified results were exported and the validated ^{14}N and ^{15}N peptide identifications were then merged to calculate peptide ratios as the mean of the individual XPRESS ratios from identified spectra. The fold change of cysteine containing peptides were corrected with the fold change of the corresponding protein expression. For the mock-treated ^{15}N- and ^{14}N- samples, 95% confidence intervals of the data were calculated by mean ± 1.96 standard deviations, which indicate the deviation caused by randomness, and they were used for cutoffs of significant alternation for both biological replicates. Only peptide/proteins identified as significant alteration from both biological replicates were reported as redox regulated peptide/proteins. The subcellular localization and biological process of the identified putative redox-sensitive proteins were predicted using SUBA (http://suba.plantenergy.uwa.edu.au/) and Gene Ontology (https://www.ebi.ac.uk/QuickGO/). Intra-molecular disulfide bonds were analyzed with the sequences of identified redox-sensitive proteins using DiANNA software (http://clavius.bc.edu/~clotelab/DiANNA/), and a (Module B) score > 0.9 was considered as significant prediction [28].

Results and Discussion

Induction of hydrogen peroxide in response to infection by *Pst*

To determine the oxidative burst following the pathogen infection, *in situ* hydrogen peroxide accumulation was detected in the leaves infected by the virulent *Pseudomonas syringae* pv. *tomato* DC3000 (*Pst*) strain and the avirulent strain expressing the avirulence gene *avrRpm1* (*Pst avrRpm1*) by 3,3′-diaminobenzidine (DAB) staining. The staining intensity indicates the amount of H_2O_2 accumulation. As shown in Figure 1, heavy brown precipitates were observed in the leaves after 30 min pathogen infection, and increased with extended time of infection. For *Pst avrRpm1* infection, H_2O_2 accumulation reached the highest level at 1-hr and 3-hr ($p<0.01$, t-test), whereas for *Pst* infection, the

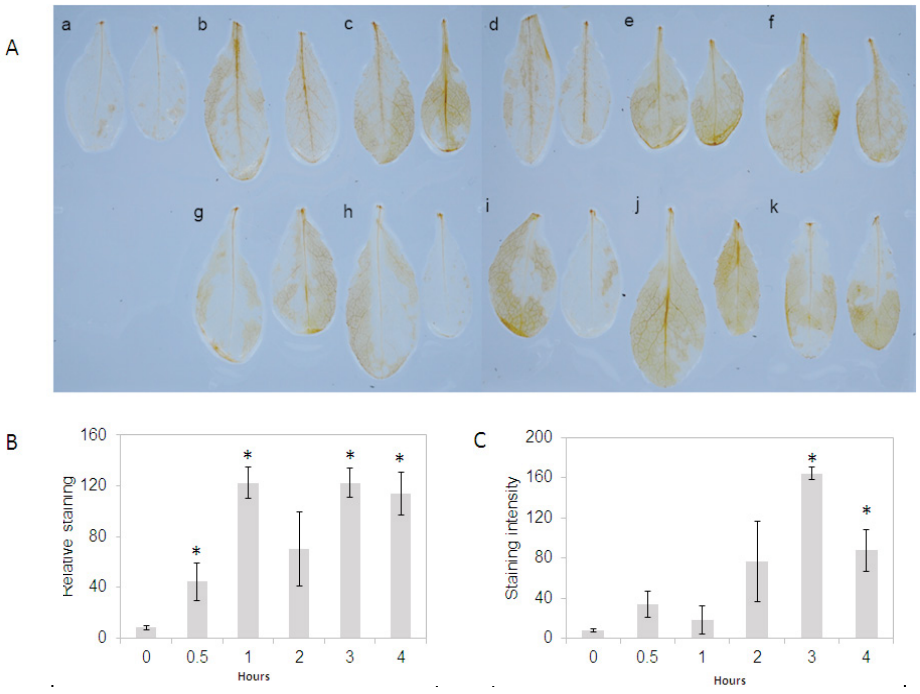

Figure 1: H_2O_2 accumulation in Arabidopsis leaves after *Pst avrRpm1* or *Pst* treatment. A, Representative of H_2O_2 accumulation in Arabidopsis leaves detected by DAB staining. a, control; b-f, *Pst avrRpm1* treatment for 0.5 hr, 1 hr, 2 hrs, 3 hrs and 4 hrs, respectively; *g-k, Pst* treatment for 0.5 hr, 1 hr, 2 hrs, 3 hrs and 4 hrs respectively. B, Comparison of DAB staining intensity after *Pst avrRpm1* treatment. C, Comparison of DAB staining intensity after *Pst* treatment. Error bars indicate ± standard deviation (n = 6). Asterisks (∗) indicate statistically significant changes compared to control ($p<0.01$, t-test).

highest H_2O_2 accumulation was at 3-hr. We collected leaves at 3 hrs post-infection by *Pst* and at 1- and 3-hr post-infection by *Pst avrRpm1* for redox-sensitive protein identification.

In vivo 15N metabolic labeling and plant pathogen infection

Previously, we developed a gel-based method as well as a gel-free proteomic approach termed OxiTRAQ [15] to identify redox-sensitive proteins in Arabidopsis suspension cells. With these approaches, more than one hundred proteins have been found to be oxidatively modified upon treatments with hydrogen peroxide, salicylate, or flg22 (a 22 amino acid peptide from bacterial pathogens flagellin) [14-16]. With chemical isotopic labeling, such as iTRAQ, different samples were combined at peptide level. The process to prepare peptides before labeling normally carries high variation among different sample, and could cause inaccurate quantitation. This motivated us to look into an *in vivo* metabolic labelling strategy in which equal amount of raw plant samples were combined after sample harvest. Subsequent protein extraction, digestion and enrichment of cysteine-containing peptides were processed with the combined sample instead of individual sample. In addition, a reciprocal-labeling strategy was applied to eliminate any isotope effects [29], also allowing us to alleviate systematic bias between different samples. The overall experimental schematic is shown in Figure 2. In the first replicate, control (mock-treated) plants grown in natural-abundance medium (^{14}N) was combined with pathogen-treated plants grown in medium that was enriched with ^{15}N heavy isotope. The second replicate was performed by combining mock-treated ^{15}N-labeled plant with pathogen-treated natural-abundance (^{14}N) plant. Therefore, any changes in redox states or protein expression level under pathogen infection would show a reciprocal ratio in the reciprocal labeling replicates. In particular, a mixture of mock-treated natural-abundance (^{14}N) plants with mock-treated ^{15}N-labeled plants at a 1:1 ratio was set to define the inherent variations of labeled and unlabeled samples in the pair wise comparison. The quantitation of redox-regulated post-translational modifications (PTMs) is based on the difference in abundance of peptides in different samples that contain reversibly oxidized thiol(s). However, such observed changes reflect not only the changes in redox status, but also the expression of corresponding proteins, thereby leading to a false interpretation in redox change. Thus, a parallel proteomic experiment was conducted in this study to determine protein expression levels for the same sample, and used for correction of the fold change of redox-sensitive peptides. It should be noted that we were interested in the proteins with altered oxidative state under pathogens infection. The discussion will be focused on the redox-sensitive proteins identified in this study.

Identification of proteins with altered redox states upon pathogen infection

In total, 2409 proteins and 387 cysteine-containing peptides were quantified in both reciprocal replicates of pathogen infection. The lists of all quantified proteins and cysteine-containing peptides/proteins in each biological replicate were presented in Supplementary Tables 1 and 2, respectively. In the 1:1 mixtures consisting of equal amounts of mock-treated ^{15}N-labeled and unlabeled samples, the results showed a normal distribution in both cysteine-containing peptides and total protein with an average ratio of 1 (Figure 3). Based on 95% confidence intervals of these data which were calculated by mean ± 1.96 standard deviations, 1.9 and 1.8 fold change were used as cut-off ratios for significantly differential expression of redox-sensitive peptides and total protein level, respectively. In addition, significantly changed proteins or peptides identified in the treatment to control samples

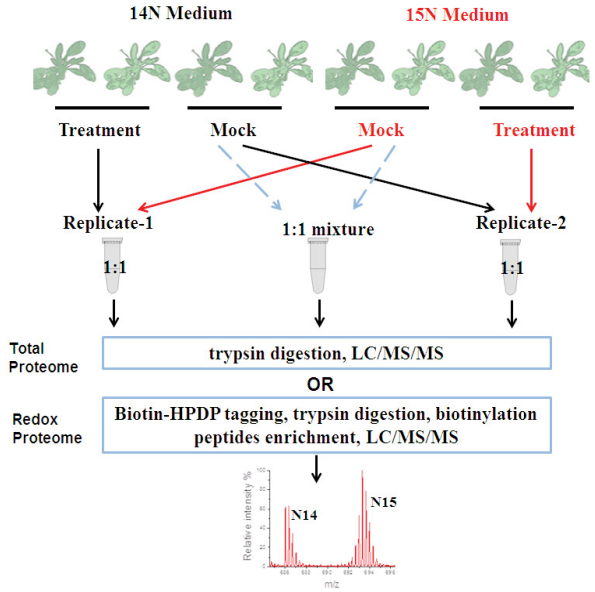

Figure 2: Experimental workflow of reciprocal nitrogen isotope labeling. Arabidopsis (Col-0) plants were grown in the presence of either ^{14}N-containing or >98% ^{15}N-enriched KNO_3 and NH_4NO_3 as sole nitrogen sources medium. In replicate 1, plants grown in ^{14}N medium were pathogen infected, whereas plants labeled with ^{15}N were treated as mock; in replicate 2, labeling was reversed. Following sample collection and mixed in equal ratios, proteins were extracted, biotin-HPDP tagged, trypsin digested, biotinylated peptides enriched and analyzed by LC-MS/MS. Mascot and XPRESS were used for protein identification and quantification. A parallel total proteome experiment was conducted to determine protein expression level for the same sample.

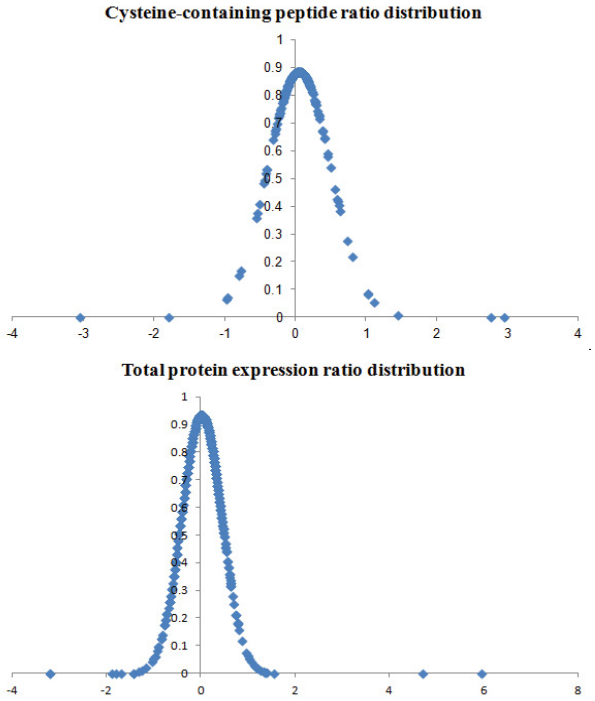

Figure 3: Ratio distribution of cysteine-containing peptides and total proteins. The log2-transformed ratios of 1:1 mixture of untreated ^{15}N-labeled and natural-abundance (^{14}N) sample showed a normal distribution, and (0.56, 1.9) and (0.57, 1.8) are the 95% confidence intervals of cysteine-containing peptides and total proteins respectively.

were compared to those identified in the 1:1 mixture of mock-treated ^{15}N-labeled and ^{14}N samples. No significant proteins were overlapped between them, which indicates that the significant proteins or peptides were not caused by technical noise. Based on these criteria, a total of 101 proteins showed significant changes at their expression levels after *Pst avrRpm1* and *Pst* treatments (Supplementary Table 3). Among them, 54 and 14 proteins were from the 1-hr and 3-hr *Pst avrRpm1* treatment, respectively, and 45 proteins from the 3-hr *Pst* treatment. Nine proteins were common in both virulent and avirulent pathogen infection, including four proteins that are known to be defense responsive: hydrogen peroxide scavenger ascorbate peroxidase APX3 [30], ILITHYIA (ILA) involved in plant immunity [31], RNA binding protein Tudor-SN 2 [32], and ACC oxidase-like protein [33]. Sixteen of the 101 proteins were annotated with stress responses, 14 of which showed up-regulated during the pathogens infection. Although there were general poor correlation in the expression between protein and RNA [34], 14 identified proteins were reported to have similarly differential changes in their transcript levels of upon *Pst* treatment in Arabidopsis [35].

To determine proteins/peptides with altered redox states, the same strategy as OxiTRAQ [15] was used that labeling cysteines before and after reduction with different cysteine-reactive reagents. After the cysteine-containing peptides' fold change was corrected to their protein expression levels, 40 peptides were identified with significantly altered abundance in protein redox state. Since some peptides are conserved among a protein family, these significant peptides represent 48 proteins in 36 non-redundant protein families (Table 1). Among them, 7 and 13 were found after 1-hr and 3-hr infection by *Pst avrRpm1*, respectively, and 39 after 3-hr infection with *Pst*. Four of them were found to altered redox states under the 3 hr infection by both *Pst avrRpm1* and *Pst*, including beta galactosidase 9, early nodulin-like protein 15 and a ribosomal L5P family protein. Among the redox-sensitive proteins, 4 of them also showed expression level changes. These included a chromosome condensation family protein (UVR8), two aspartyl protease family proteins and translation initiation factor 2 subunit 1. The rest 90% of the redox-regulated proteins were modified only at the PTMs level instead of protein expression levels. Thirteen of the redox-sensitive proteins identified from this study have been reported to be redox-regulated, including tryptophan synthase beta type 2 [36], a cysteine proteinase superfamily protein [37], a glutathione S-transferase family protein [38] and chaperonin 60 beta [39] (Supplementary Table 4).

Furthermore, 18 of the 40 redox-sensitive peptides were predicted to form intra-molecular disulfide bonds (Table 1). It should be noted that besides disulfide bonds, other reversible modifications (S-nitrosylation, glutathionylation and sulfenic acid) are also chemically reversible. The reversible thiol modifications identified in this study could be due to any of those types of modifications.

Protein ID[a)]	Protein description	Functional categorization	Localization	Peptide sequence	Normalized ratio	DiANNA[b)]
***Pst avrRpm1*-1 hr**						
AT1G78060.1	Glycosyl hydrolase family protein	Cell wall organization and biogenesis	extracellular	K.TLLGNYAGPPCK.T	9.22	✓
AT5G38530.1	TSBtype2|tryptophan synthase beta type 2	cellular metabolic process	plastid	R.AVEPSACPSLTK.G	1.98	
ATCG00470.1	ATPE|ATP synthase epsilon chain	transport	plastid	M.TLNLCVLTPNR.L	3.63	
AT1G68010.1,AT1G68010.2	ATHPR1|hydroxypyruvate reductase	others	peroxisome	R.WINLLVDQGCR.V	2.44	
AT1G73060.1	LPA3|Low PSII Accumulation 3	Chloroplast organization or photosynthesis	plastid	K.QTDGSFACVAESPTR.F	0.48	
AT1G30360.1	ERD4|Early-responsive to dehydration stress protein (ERD4)	stress response	plasma membrane	K.TGFCGLVGK.Q	2.89	✓
***Pst avrRpm1*-3 hr**						
AT2G32810.1,AT2G32810.2	BGAL9|beta galactosidase 9	Cell wall organization and biogenesis	vacuole	R.GSCDGFSIGK.C	0.12	
AT4G31840.1	ENODL15|early nodulin-like protein 15	other	extracellular	K.LDQAGPVYFVSGTEGHCQK.G	2.25	
AT5G63860.1	UVR8|Regulator of chromosome condensation (RCC1) family protein	stress response	cytosol,nucleus	K.VVQVSCGWR.H	0.47	
AT3G18490.1	ASPG1|Eukaryotic aspartyl protease family protein	proteolysis	extracellular	K.SLTCSAPQCSLLETSACR.S	0.55	✓
AT1G02305.1	Cysteine proteinases superfamily protein	proteolysis	vacuole	R.TAWSQCTSIGR.L	2.32	
ATCG00470.1	ATPE|ATP synthase epsilon chain	transport	plastid	M.TLNLCVLTPNR.L	1.91	
AT4G01310.1	Ribosomal L5P family protein	translation	plastid	K.IVVNCGIGDAAQNDK.G	2.03	
AT1G54500.1	Rubredoxin-like superfamily protein	Chloroplast organization or photosynthesis	plastid	K.FAVLNTGIYECR.S	0.48	
AT4G19880.1,AT4G19880.2,AT4G19880.3	Glutathione S-transferase family protein	stress response	plastid	R.YICGNTLTETDIR.L	1.98	
AT1G21670.1	DPP6 amino-terminal domain protein	Cell wall organization and biogenesis	extracellular	R.FGPSCSIQDFK.T	2.21	
***Pst* -3 hr**						
AT5G27540.1,AT5G27540.2	MIRO1|MIRO-related GTP-ase 1	others	mitochondrion	R.YAAGAVDCPGSPK.S	2.96	

AT5G19620.1	ATOEP80|outer envelope protein of 80 kDa	Chloroplast organization or photosynthesis	plastid	R.GLVCENANVLPSK.F	0.15	✓
AT3G10380.1	SEC8|subunit of exocyst complex 8	transport	cytosol	K.VAAAGAIICQK.L	0.31	
AT3G52960.1	Thioredoxin superfamily protein	stress response	plastid	K.KTILFAVPGAFTPTCSQK.H	2.08	
AT2G27680.1	NAD(P)-linked oxidoreductase superfamily protein	others	plastid	R.MAQLCELTGVK.L	1.95	
AT5G08280.1	HEMC|hydroxymethylbilane synthase	cellular metabolic process	plastid	R.AFLETLDGSCR.T	0.51	✓
AT5G51970.1,AT5G51970.2	putative sorbitol dehydrogenase	cellular metabolic process	cytosol	K.AVGICGSDVHYLK.T	0.51	✓
AT4G32520.1,AT4G32520.2	SHM3|serine hydroxymethyltransferase 3	cellular metabolic process	plastid	R.AVMEAVGSCLTNK.Y	1.92	
AT3G13750.1	BGAL1|beta galactosidase 1	Cell wall organization and biogenesis	extracellular	K.FASFGTPEGTCGSYR.Q	2.01	✓
AT3G13750.1	BGAL1|beta galactosidase 1	Cell wall organization and biogenesis	extracellular	K.SGACSAFLANYNPK.S	2.04	
AT2G32810.1,AT2G32810.2	BGAL9|beta galactosidase 9	Cell wall organization and biogenesis	vacuole	R.GSCDGFSIGK.C	0.27	✓
AT5G63800.1	BGAL6|Glycosyl hydrolase family 35 protein	Cell wall organization and biogenesis	extracellular	K.VQISCGGTKPIDLSR.S	3.5	
AT3G06510.1,AT3G06510.2	SFR2|Glycosyl hydrolase superfamily protein	Chloroplast organization or photosynthesis	plastid	K.ETPCSAEEAEAADKK.A	4.35	
AT1G78060.1	Glycosyl hydrolase family protein	Cell wall organization and biogenesis	extracellular	K.TLLGNYAGPPCK.T	8.58	✓
AT1G78060.1	Glycosyl hydrolase family protein	Cell wall organization and biogenesis	extracellular	R.VNGIPSCADPNLLTR.T	8.59	✓
AT1G78060.1	Glycosyl hydrolase family protein	Cell wall organization and biogenesis	extracellular	K.AGMDVNCGSYLQK.H	6.04	✓
AT5G04360.1	ATLDA|limit dextrinase	cellular metabolic process	plastid	K.LETCYANDPYAR.G	2.04	
AT1G05850.1	ATCTL1|Chitinase family protein	Cell wall organization and biogenesis	plasma membrane	K.YPCSPGAEYYGR.G	2.36	✓
AT2G42910.1	Phosphoribosyltransferase family protein	cellular metabolic process	cytosol	K.LLDHYPTVVCTK.V	2.5	
AT4G31840.1	ENODL15|early nodulin-like protein 15	others	extracellular	K.LDQAGPVYFVSGTEGHCQK.G	3.23	
AT4G24220.1,AT4G24220.2	VEP1|NAD(P)-binding Rossmann-fold superfamily protein	cellular metabolic process	peroxisome	K.NEAFNCNNADIFK.W	2.16	✓
AT2G40290.1,AT2G40290.2,AT2G40290.3	Eukaryotic translation initiation factor 2 subunit 1	translation	cytosol	R.VSEEDIQTCEER.Y	2.69	✓
AT4G01310.1	Ribosomal L5P family protein	translation	plastid	K.IVVNCGIGDAAQNDK.G	3.08	
AT3G52500.1	Eukaryotic aspartyl protease family protein	proteolysis	extracellular	R.YLCSGCDFSGLDPTLIPR.F	3.65	✓
AT1G55490.1,AT1G55490.2	CPN60B|chaperonin 60 beta	others	plastid	K.MSVEFDNCK.L	2.17	
AT4G12830.1	HCF101|protein high chlorophyll fluorescence 101	Chloroplast organization or photosynthesis	plastid	R.ASDKPLTSCGPYK.M	6.38	
AT3G24430.1	HCF101|protein high chlorophyll fluorescence 101	Chloroplast organization or photosynthesis	plastid	R.ISNIIAVSSCK.G	3.03	✓
AT1G73060.1	LPA3|Low PSII Accumulation 3	Chloroplast organization or photosynthesis	plastid	K.QTDGSFACVAESPTR.F	0.55	
AT1G30360.1	ERD4|Early-responsive to dehydration stress protein (ERD4)	stress response	plasma membrane	K.TGFCGLVGK.Q	2.14	✓
AT5G65810.1	CGR3|cotton Golgi-related 3	Cell wall organization and biogenesis	golgi	K.ITGDYSCTAEVQR.A	2.96	✓

a) Proteins regulated in both DC3000 and *avrRpm*1 treated samples are marked in bold.
b) Prediction of intra-molecular disulfide bond formation by DiANNA

Table 1: The list of putative redox-sensitive peptides upon pathogen infection.

Categorization of pathogen-responsive redox-sensitive proteins

Subcellular localization: The subcellular localization of the redox-sensitive proteins and differentially expressed proteins was categorized based on Gene Ontology annotation (Figure 4 and Supplementary Figure). As for the differentially expressed proteins, the top two localization categories are plastid and cytosol, whereas plastid and extracellular proteins represent the top localization categories for redox-sensitive proteins. It is well-known that redox regulation occurs in chloroplast including the light-dependent thiol-disulfide exchange [12].

Biological processes: The top three enriched biological processes for the differentially expressed proteins are cellular metabolic processes, stress response, and redox regulation/transport. In the redox-sensitive protein group, the cell wall organization and biogenesis, cellular

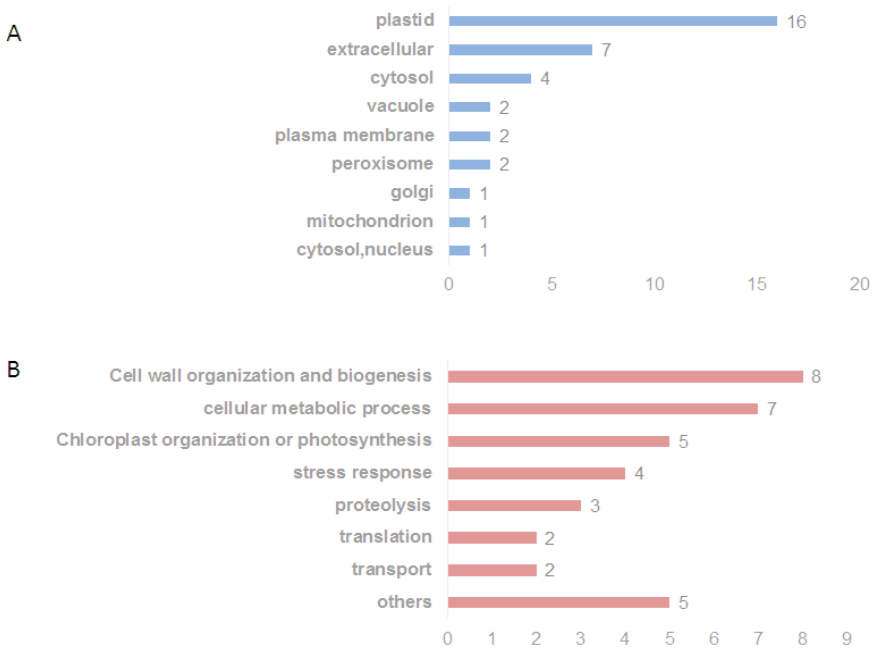

Figure 4: Subcellular localization and biological process categorization of pathogen-responsive redox-sensitive proteins. The subcellular localization and biological process GO terms are shown on the y-axis. Numbers of proteins with a significant change in their redox states in each category are shown on the x-axis.

metabolic process, and photosynthesis represent top three enriched GO terms.

Cell wall organization and biogenesis: Plant cell wall serves the first line of defense against pathogens [40]. A number of studies on cell wall proteome during bacterial pathogen infection have mainly focused on plant cell cultures but not with plant tissue [41]. In this study, we found seven proteins involved in cell wall organization and biogenesis were redox-sensitive in Arabidopsis plant tissue. These include three beta galactosidases (BGALs), a glycosyl hydrolase family protein, a chitinase-like protein AtCTL1, Golgi-related 3 (CGR3), and DPP6 amino-terminal domain protein. The plant β-galactosidases are essential in the metabolism of galactosyl conjugates during carbohydrate reserve mobilization and cell wall expansion and degradation [42,43]. The Arabidopsis genome contains 17 predicted β-galactosidase genes, designated as BGAL1–17 [44]. BGAL1, BGAL6 and BGAL9 were identified in this study. BGAL1 and BGAL6 became oxidized after 3 hrs of virulent pathogen treatment, while BGAL9 was reduced in both virulent and avirulent pathogen infection. Deletion of BGAL6 was reported to affect extrude mucilage from the apoplast upon hydration [45]. In *Escherichia coli*, it was reported that β-galactosidase could form disulfide bond to active its function under oxidizing conditions *in vitro* [46]. However, the majority of plant BGALs' function are not characterized. The change of BGALs's redox states upon pathogen infection indicates their involvement in plant defense response through oxidative modifications. Three cysteine-containing peptides in the glycosyl hydrolase family protein were oxidized upon pathogen treatments. These three peptides were all predicted to form intra-molecular disulfide bonds. Earlier, hydrolase family was showed to be regulated at gene's transcription level during geminivirus infection [47]. Thus, this gene/protein family contributes to plant defense response not only at the transcription level, but also as protein redox switch.

Cellular metabolism and photosynthesis: Metabolic reprogramming is essential to balance defense and growth. Earlier studies have suggested that many starch metabolic enzymes are redox-regulated [48]. In the study, we identified a redox-sensitive protein limit dextrinase (AtLDA) that has a role in the hydrolysis of the α-1,6 linkages during starch degradation. In agreement with our study, this protein has been previously identified as redox-sensitive in spinach [49] and wheat [50]. The putative sorbitol dehydrogenase was also found to be S-glutathionyled in Arabidopsis under *tert*-butylhydroperoxide treatment [51]. Chloroplasts are key players in plant defense. The loss of integrity of PSII may lead to the HR-associated oxidative burst. Many redox-sensitive proteins in chloroplasts regulate enzyme activity in response to stresses by reduction of regulatory disulfides in target enzymes, ensuring coordination between photosynthesis and energy production [48]. Six proteins involved in photosynthesis were found redox-modified. Of these, 3 proteins were in more reduced states, including outer envelope protein of 80 kDa, rubredoxin-like superfamily protein, and low PSII Accumulation 3, and two proteins were more oxidized including high chlorophyll fluorescence 101 (HCF101) and hydroxypyruvate reductase. Rubredoxins are [1Fe-0S] proteins in which one iron atom is coordinated by four cysteine residues. Many studies have reported that rubredoxins act as electron carriers in a variety of biochemical processes including detoxification of reactive oxygen species [52,53] and fatty acid metabolism [54]. The protein HCF101 has been shown to be essential for the accumulation of the membrane complex photosystem I and the soluble ferredoxin-thioredoxin reductases [55]. The redox-sensitive cysteine residue (underlined) identified in this study is present in the highly conserved P-loop domain of the plant HCF101 (ISNIIAVSSCK), and it was predicted to form an intra-molecular disulfide bond.

Other biological processes: The other redox-sensitive proteins were classified into stress responses, proteolysis, transport, translation and development. Among them, early-responsive to dehydration stress protein (ERD4) was identified as a part of the chloroplast envelope

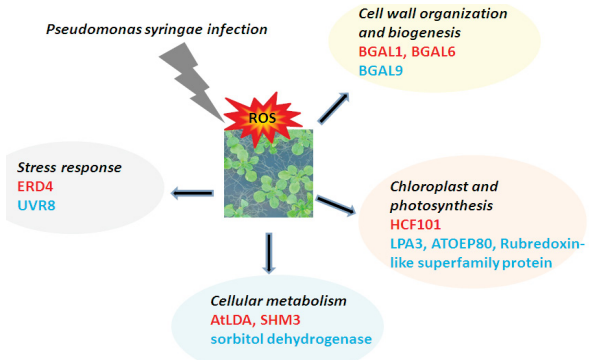

Figure 5: Schematic representation of redox-sensitive proteins involved in pathogen infection. Oxidized and reduced proteins are indicated by red and green color, respectively. Under the *Pseudomonas syringae* infection, ROS were over produced in the plant cells. A number of redox-sensitive proteins were identified in this process and involved in various biological processes as presented in the oval spheres. BGALs, beta galactosidases; HCF101, high chlorophyll fluorescence 101; LPA3, low PSII accumulation 3; ATOEP80, outer envelope protein of 80 kDa; AtLDA, limit dextrinase; SHM3, serine hydroxymethyltransferase 3; ERD4, early-responsive to dehydration stress protein; UVR8, UV-B resistance 8.

proteome [56] with function in the early stages of plant adaptation to abiotic stress conditions [57]. EDR4 identified as a redox-sensitive protein upon the pathogen attack suggests its function in plant defense. UV resistance locus 8 (UVR8) with sequence similarity to the eukaryotic guanine nucleotide exchange factor RCC1, is located in the nucleus and associates with chromatin in the HY5 promoter region to regulate the protective gene expression [58]. It was also up-regulated in Arabidopsis plants grown under salt or osmotic stress conditions [59]. UV exposure, like pathogen infection, causes ROS stress and UVB8 could play a similar role during these oxidative stresses through its oxidative modification. Other proteins identified in the study include putative cathepsin B-like cysteine protease that functions in basal defense response as well as a potential regulatory role in distinct forms of plant programmed cell death [60], endochitinase-like protein AtCTL1 with a key role in tolerance to heat, salt and drought stresses [61], and a thioredoxin superfamily protein that was reported to be S-nitrosylated in Arabidopsis undergoing hypersensitive response [62].

Conclusion

During plant-pathogen interactions, plants have evolved intricate mechanisms to recognize and trigger effective innate immune responses. ROS is an essential regulator in activation of the immune response but the mechanisms by which ROS regulate immunity remains largely unknown. Using *in vivo* metabolic labeling proteomics method combined with biotin-switch technique, we identified a number of proteins with altered redox states in Arabidopsis plants upon infection by virulent and avirulent pathogens. Many of the redox-sensitive proteins identified in this study have not been recognized previously to undergo oxidative modifications. These redox-regulated proteins are involved in cell wall organization and biogenesis and in chloroplast function in addition to other biological pathways (Figure 5). These results have expanded our knowledge of proteins redox switch during plant-pathogen interactions and the knowledge will help for future study toward understanding the plant defense mechanisms.

Acknowledgement

This work was supported by Research Grants Council of Hong Kong (grant no. HKBU1/CRF/10 and HKBU261910 to Y.X.).

References

1. Boller T, Felix G (2009) A renaissance of elicitors: perception of microbe-associated molecular patterns and danger signals by pattern-recognition receptors. Annu Rev Plant Biol 60: 379-406.
2. Robert-Seilaniantz A, Grant M, Jones JD (2011) NHormone crosstalk in plant disease and defense: more than just jasmonate-salicylate antagonism. Annu Rev Phytopathol 49: 317-343.
3. Dangl JL, Jones JDG (2001) Plant pathogens and integrated defence responses to infection. Nature 411: 826-833.
4. Katagiri F, Thilmony R, He SY (2002) The Arabidopsis thaliana-pseudomonas syringae interaction. Arabidopsis Book 1: e0039.
5. Apel K, Hirt H (2004) Reactive oxygen species: metabolism, oxidative stress, and signal transduction. Annu Rev Plant Biol 55: 373-399.
6. Levine A, Tenhaken R, Dixon R, Lamb C (1994) H_2O_2 from the oxidative burst orchestrates the plant hypersensitive disease resistance response. Cell 79: 583-593.
7. Chinchilla D, Zipfel C, Robatzek S, Kemmerling B, Nurnberger T, et al. (2007) A flagellin-induced complex of the receptor FLS2 and BAK1 initiates plant defence. Nature 448: 497-500.
8. Torres MA, Jones JD, Dangl JL (2006) Reactive oxygen species signaling in response to pathogens. Plant Physiol 141: 373-378.
9. Orozco-Cardenas ML, Narvaez-Vasquez J, Ryan CA (2001) Hydrogen peroxide acts as a second messenger for the induction of defense genes in tomato plants in response to wounding, systemin, and methyl jasmonate. Plant Cell 13: 179-191.
10. Poole LB, Nelson KJ (2008) Discovering mechanisms of signaling-mediated cysteine oxidation. Curr Opin Chem Biol 12: 18-24.
11. Green J, Paget MS (2004) Bacterial redox sensors. Nat Rev Microbiol 2: 954-966.
12. Balsera M, Uberegui E, Schurmann P, Buchanan BB (2014) Evolutionary development of redox regulation in chloroplasts. Antioxid Redox Signal 21: 1327-1355.
13. Spadaro D, Yun BW, Spoel SH, Chu C, Wang YQ, et al. (2010) The redox switch: dynamic regulation of protein function by cysteine modifications. Physiol Plant 138: 360-371.
14. Wang H, Wang S, Lu Y, Alvarez S, Hicks LM, et al. (2012) Proteomic analysis of early-responsive redox-sensitive proteins in Arabidopsis. J Proteome Res 11: 412-424.
15. Liu P, Zhang H, Wang H, Xia Y (2013) Identification of redox-sensitive cysteines in the Arabidopsis proteome using oxitraq, a quantitative redox proteomics method. Proteomics 14: 750-762.
16. Liu P, Zhang H, Yu B, Xiong L, Xia Y, et al. (2015) Proteomic identification of early salicylate- and flg22-responsive redox-sensitive proteins in Arabidopsis. Sci Rep 5: 8625.
17. Mou Z, Fan W, Dong X (2003) Inducers of plant systemic acquired resistance regulate NPR1 function through redox changes. Cell 113: 935-944.
18. Lindermayr C, Sell S, Muller B, Leister D, Durner J, et al. (2010) Redox regulation of the NPR1-TGA1 system of Arabidopsis thaliana by nitric oxide. Plant Cell 22: 2894-2907.
19. Yun BW, Feechan A, Yin M, Saidi NB, Le Bihan T, et al. (2011) S-nitrosylation of NADPH oxidase regulates cell death in plant immunity. Nature 478: 264-268.
20. Wang YQ, Feechan A, Yun BW, Shafiei R, Hofmann A, et al. (2009) S-nitrosylation of AtSABP3 antagonizes the expression of plant immunity. J Biol Chem 284: 2131-2137.
21. Balmant KM, Parker J, Yoo MJ, Zhu N, Dufresne C, et al. (2015) Redox proteomics of tomato in response to Pseudomonas syringae infection. Horticulture Research 2:15043.
22. Akter S, Huang J, Waszczak C, Jacques S, Gevaert K, et al. Cysteines under ROS attack in plants: a proteomics view. J Exp Bot 66: 2935-2944.
23. Mock HP, Dietz KJ (2016) Redox proteomics for the assessment of redox-related posttranslational regulation in plants. Biochim Biophys Acta 8: 967-973.
24. Dangl JL, Ritter C, Gibbon MJ, Mur LA, Wood JR, et al. (1992) Functional

homologs of the Arabidopsis RPM1 disease resistance gene in bean and pea. Plant Cell 4: 1359-1369.

25. Thordal-Christensen H, Zhang Z, Wei Y, Collinge DB (1997) Subcellular localization of H_2O_2 in plants. H_2O_2 accumulation in papillae and hypersensitive response during the barley—powdery mildew interaction. The Plant Journal 11: 1187-1194.

26. Lamesch P, Berardini TZ, Li D, Swarbreck D, Wilks C, et al. (2012) The Arabidopsis Information Resource (TAIR): improved gene annotation and new tools. Nucleic Acids Res 40: D1202-D1210.

27. Perkins DN, Pappin DJ, Creasy DM, Cottrell JS (1999) Probability-based protein identification by searching sequence databases using mass spectrometry data. Electrophoresis 20: 3551-3567.

28. Ferre F, Clote P (2005) DiANNA: a web server for disulfide connectivity prediction. Nucleic Acids Res 2005 33: W230-W232.

29. Arsova B, Kierszniowska S, Schulze WX (2012) The use of heavy nitrogen in quantitative proteomics experiments in plants. Trends Plant Sci 17: 102-112.

30. Caverzan A, Passaia G, Rosa SB, Ribeiro CW, Lazzarotto F, et al. (2012) Plant responses to stresses: Role of ascorbate peroxidase in the antioxidant protection. Genet Mol Biol 35: 1011-1019.

31. Monaghan J, Li X (2010) The HEAT repeat protein ILITYHIA is required for plant immunity. Plant Cell Physiol 51: 742-753.

32. dit Frey NF, Muller P, Jammes F, Kizis D, Leung J, et al. (2010) The RNA binding protein Tudor-SN is essential for stress tolerance and stabilizes levels of stress-responsive mRNAs encoding secreted proteins in Arabidopsis. Plant Cell 22: 1575-1591.

33. Hansen BG, Kerwin RE, Ober JA, Lambrix VM, Mitchell-Olds T, et al. (2008) A novel 2-oxoacid-dependent dioxygenase involved in the formation of the goiterogenic 2-hydroxybut-3-enyl glucosinolate and generalist insect resistance in Arabidopsis. Plant Physiol 148: 2096-2108.

34. Maier T, Guell M, Serrano L (2009) Correlation of mRNA and protein in complex biological samples. FEBS Lett 583: 3966-3973.

35. Bolivar JC, Machens F, Brill Y, Romanov A, Bulow L, et al. (2014) 'In silico expression analysis', a novel PathoPlant web tool to identify abiotic and biotic stress conditions associated with specific cis-regulatory sequences. Database. 2014: bau030.

36. Balmer Y, Vensel WH, Cai N, Manieri W, Schurmann P, et al. (2006) A complete ferredoxin/thioredoxin system regulates fundamental processes in amyloplasts. Proc Natl Acad Sci U S A 103: 2988-2993.

37. Bocedi A, Gradoni L, Menegatti E, Ascenzi P (2004) Kinetics of parasite cysteine proteinase inactivation by NO-donors. Biochem Biophys Res Commun 315: 710-718.

38. Marchand C, Marechal PL, Meyer Y, Miginiac-Maslow M, Issakidis-Bourguet E, et al. (2004) New targets of Arabidopsis thioredoxins revealed by proteomic analysis. Proteomics 4: 2696-2706.

39. Yamazaki D, Motohashi K, Kasama T, Hara Y, Hisabori T, et al. (2004) Target proteins of the cytosolic thioredoxins in Arabidopsis thaliana. Plant Cell Physiol 45: 18-27.

40. Malinovsky FG, Fangel JU, Willats WG (2014) The role of the cell wall in plant immunity. Front Plant Sci 5.

41. O'Brien JA, Daudi A, Butt VS, Bolwell GP (2012) Reactive oxygen species and their role in plant defence and cell wall metabolism. Planta 236: 765-779.

42. de Alcantara PH, Martim L, Silva CO, Dietrich SM, Buckeridge MS, et al. (2006) Purification of a beta-galactosidase from cotyledons of *Hymenaea courbaril L.* (*Leguminosae*). Enzyme properties and biological function. Plant Physiol Biochem 44: 619-627.

43. Esteban R, Dopico B, Munoz FJ, Romo S, Martin I, et al. (2003) Cloning of a Cicer arietinum beta-galactosidase with pectin-degrading function. Plant Cell Physiol 44: 718-725.

44. Yang J, Carroll KS, Liebler DC (2016) The Expanding Landscape of the Thiol Redox Proteome. Mol Cell Proteomics 15: 1-11.

45. Dean GH, Zheng H, Tewari J, Huang J, Young DS, et al. (2007) The Arabidopsis MUM2 gene encodes a beta-galactosidase required for the production of seed coat mucilage with correct hydration properties. Plant Cell 19: 4007-4021.

46. Seras-Franzoso J, Affentranger R, Ferrer-Navarro M, Daura X, Villaverde A, et al. (2012) Disulfide bond formation and activation of Escherichia coli beta-galactosidase under oxidizing conditions. Appl Environ Microbiol 78: 2376-2385.

47. Ascencio-Ibanez JT, Sozzani R, Lee TJ, Chu TM, Wolfinger RD, et al. (2008) Global analysis of Arabidopsis gene expression uncovers a complex array of changes impacting pathogen response and cell cycle during geminivirus infection. Plant Physiol 148: 436-454.

48. Glaring MA, Skryhan K, Kotting O, Zeeman SC, Blennow A, et al. (2012) Comprehensive survey of redox sensitive starch metabolising enzymes in *Arabidopsis thaliana*. Plant Physiol Biochem 58: 89-97.

49. Schindler I, Renz A, Schmid FX, Beck E (2001) Activation of spinach pullulanase by reduction results in a decrease in the number of isomeric forms. Biochim Biophys Acta 13: 175-186.

50. Repellin A, Båga M, Chibbar RN (2008) *In vitro* pullulanase activity of wheat (*Triticum aestivum L.*) limit-dextrinase type starch debranching enzyme is modulated by redox conditions. J Cereal Sci 47: 302-309.

51. Dixon DP, Skipsey M, Grundy NM, Edwards R (2005) Stress-induced protein S-glutathionylation in Arabidopsis. Plant Physiol 138: 2233-2244.

52. Fritsch J, Lenz O, Friedrich B (2011) The maturation factors HoxR and HoxT contribute to oxygen tolerance of membrane-bound [NiFe] hydrogenase in *Ralstonia eutropha* H16. J Bacteriol 193: 2487-2497.

53. Kurtz DM (2004) Microbial detoxification of superoxide: the non-heme iron reductive paradigm for combating oxidative stress. Acc Chem Res 37: 902-908.

54. Calderon RH, Garcia-Cerdan JG, Malnoe A, Cook R, Russell JJ, et al. (2013) A conserved rubredoxin is necessary for photosystem II accumulation in diverse oxygenic photoautotrophs. J Biol Chem 288: 26688-26696.

55. Schwenkert S, Netz DJ, Frazzon J, Pierik AJ, Bill E, et al. (2009) Chloroplast HCF101 is a scaffold protein for [4Fe-4S] cluster assembly. Biochem J 425: 207-218.

56. Froehlich JE, Wilkerson CG, Ray WK, McAndrew RS, Osteryoung KW, et al. (2003) Proteomic Study of the Arabidopsis thaliana Chloroplastic Envelope Membrane Utilizing Alternatives to Traditional Two-Dimensional Electrophoresis. J Proteome Res 2: 413-425.

57. Liu Y, Li H, Shi Y, Song Y, Wang T, et al. (2009) A Maize Early Responsive to Dehydration Gene, ZmERD4, Provides Enhanced Drought and Salt Tolerance in Arabidopsis. Plant Mol Biol Rep 27: 542-548.

58. Brown BA, Cloix C, Jiang GH, Kaiserli E, Herzyk P, et al. (2005) A UV-B-specific signaling component orchestrates plant UV protection. Proc Natl Acad Sci U S A 102: 18225-18230.

59. Fasano R, Gonzalez N, Tosco A, Dal Piaz F, Docimo T, et al. (2014) Role of Arabidopsis UV RESISTANCE LOCUS 8 in Plant Growth Reduction under Osmotic Stress and Low Levels of UV-B. Molecular Plant 7: 773-791.

60. McLellan H, Gilroy EM, Yun BW, Birch PR, Loake GJ, et al. (2009) Functional redundancy in the Arabidopsis Cathepsin B gene family contributes to basal defence, the hypersensitive response and senescence. New Phytol 183: 408-418.

61. Kwon Y, Kim SH, Jung MS, Kim MS, Oh JE, et al. (2007) Arabidopsis hot2 encodes an endochitinase-like protein that is essential for tolerance to heat, salt and drought stresses. Plant J 49: 184-193.

62. Romero-Puertas MC, Campostrini N, Matte A, Righetti PG, Perazzolli M, et al. (2008) Proteomic analysis of S-nitrosylated proteins in Arabidopsis thaliana undergoing hypersensitive response. Proteomics 8: 1459-1469.